Long, S.P., 2018, Geometry and magnitude of extension in the Basin and Range Province (39°N), Utah, Nevada, and California, USA: Constraints from a province-scale cross section: GSA Bulletin, https://doi.org/10.1130/B31974.1.

Data Repository

Plate DR1. Geologic cross section across the Basin and Range Province at ~39°N (1:200,000-scale). The present-day geometry is shown on A, and the pre-extensional geometry is shown on B. See the text for details on restoration methodology and estimation of extension. Light shaded areas above the modern surface on A represent eroded rock. The present-day and restored positions of the Paleogene unconformity, which is the datum used to restore extension, are shown with thick red lines. On B, the Paleogene unconformity is restored to an elevation of ~3 km, and light shaded areas above the unconformity either represent eroded pre-Paleogene rocks or Paleogene and younger rocks deposited above the unconformity. On B, the restored positions of the modern erosion surface are shown with thick blue lines. Crustal thickness data from proximal EarthScope USArray seismic stations distributed along the length of the cross section (Gilbert, 2012) are shown on A. Interpretations of Moho depth and prominent reflectors from the COCORP seismic reflection profile are also shown on A, and are modified from Allmendinger et al. (1983) for western Utah, Hauser et al. (1987) for eastern Nevada, Allmendinger et al. (1987) for central Nevada, and Surpless et al. (2002) for western Nevada and eastern California. The COCORP data illustrate important aspects of crustal structure, but were not used for the calculation of pre-extensional thicknesses, as they were collected from ~100 km to the north of the section line across much of Nevada (see Fig. 1A in the main text).

Figure DR1. Geologic map of part of the northern Pancake Range (1:12,000-scale), mapped by S. Long. Location of cross section line is shown with dark gray line.

Table DR1. Data supporting three-point problems for determination of fault and unconformity dip angles. The ‘strike azimuth’ was determined by locating two points of equal elevation along a fault trace, and connecting them with a line. The ‘elevation difference’ column represents the vertical distance between the elevation that the strike azimuth was determined at and a lower-elevation point measured along the fault trace, which was typically located at the bottom of a drainage. The ‘horizontal distance’ column represents the map distance between the strike azimuth line and the lower-elevation point, measured perpendicular from the strike azimuth line. The ‘fault dip angle’ was calculated by the equation: dip angle = $\tan^{-1}$(elevation difference/horizontal distance).

REFERENCES CITED

Allmendinger, R.W., Sharp, J.W., Von Tish, D., Serpa, L., Brown, L., Kaufman, S., and Oliver, J., 1983, Cenozoic and Mesozoic structure of the eastern Basin and Range Province, Utah, from COCORP seismic-reflection data: Geology, v. 11, p. 532–536, https://doi.org/10.1130/0091-7613(1983)11<532:CAMSOT>2.0.CO;2.

Allmendinger, R.W., Hauge, T., Hauser, E.C., Potter, C.J., Klemperer, S.L., Nelson, D.K., Knuepfer, P., and Oliver, J., 1987, Overview of the COCORP 40°N transect, western United States; the fabric of an orogenic belt: Geological Society of America Bulletin, v. 98, p. 308–319, https://doi.org/10.1130/0016-7606(1987)98<308:OOTCNT>2.0.CO;2.

Brokaw, A.L., 1967, Geologic map and sections of the Ely quadrangle, White Pine County, Nevada: U.S. Geological Survey Geologic Quadrangle Map GQ-697, scale 1:24,000, 1 sheet.

Brokaw, A.L., and Heidrick, T., 1966, Geologic map and sections of the Giroux Wash quadrangle, White Pine County, Nevada: U.S. Geological Survey Geologic Quadrangle Map I-449, scale 1:24,000, 1 sheet.

Drewes, H., 1967, Geology of the Connors Pas quadrangle, Schell Creek Range, east-central Nevada: U.S. Geological Survey Professional Paper 557, scale 1:48,000, 1 sheet, 93 p.

Ferguson, H.G., and Cathcart, S.H., 1954, Geologic map of the Round Mountain quadrangle, Nevada: U.S. Geological Survey Geologic Quadrangle Map 40, scale 1:125,000, 1 sheet.

Gilbert, H., 2012, Crustal structure and signatures of recent tectonism as influenced by ancient terranes in the western United States: Geosphere, v. 8, p. 141–157, https://doi.org/10.1130/GES00720.1.

Hauser, E., Potter, C., Hauge, T., Burgess, S., Burtch, S., Mutschler, J., Allmendinger, R., Brown, L., Kaufman, S., and Oliver, J., 1987, Crustal structure of eastern Nevada from COCORP deep seismic reflection data: Geological Society of America Bulletin, v. 99, p. 833–844, doi:https://doi.org/10.1130/0016-7606(1987)99<833:CSOENF>2.0.CO;2.

Lohr, L.S., 1965, Geology of the Brock Canyon area, Monitor Range, Eureka County, Nevada [M.S. thesis]: Reno, University of Nevada, Reno, 44 p., 2 plates.

McKee, E.H., and Conrad, J.E., 1998, Geologic Map of the Frazier Creek Quadrangle, Nevada: Nevada Bureau of Mines and Geology Field Studies Map 15, scale 1:24,000, 1 sheet.

Schalla, R.A., 1978, Paleozoic stratigraphy of the southern Mahogany Hills, Eureka County, Nevada [M.S. thesis]: Corvallis, Oregon State University, 118 p., 6 plates.

Silberling, N.J., and John, D.A., 1989, Geologic map of pre-Tertiary rocks of the Paradise Range and southern Lodi Hills, west-central Nevada: U.S. Geological Survey Miscellaneous Field Studies Map MF-2062, scale 1:24,000, 1 sheet.

Surpless, B.E., Stockli, D.F., Dumitru, T.A., and Miller, E.L., 2002, Two-phase westward encroachment of Basin and Range extension into the northern Sierra Nevada: Tectonics, v. 21, no. 1, https://doi.org/10.1029/2000TC001257.

A. Deformed

Plate DR1: Geologic cross section across the Basin and Range Province at approximately 39°N

Scale: 1:200,000

0 5 10 15 20 25 km

No vertical exaggeration

Structure abbreviations:

CRT	Canyon Range thrust
GNT	Gunnison thrust
GT	Golconda thrust
NSRD	Northern Snake Range decollement
PVT	Pavant thrust
PXT	Paxton thrust
RMT	Roberts Mountains thrust
SDD	Sevier Desert detachment

Well abbreviations:

1	Phillips 1 US "E"
2	Mobil Larson
3	Chevron USA Chriss Canyon
4	Amoco Silver Bridge
5	Placid WXC Barton
6	Placid Monroe
7	Placid Henley
8	Cominco-American
9	Eskdale 1-25
10	Eskdale Federal 1-23
11	Baker Creek Unit 1
12	Bastian Creek Number 1
13	Titan Federal Number 1-9
14	Nevada-Federal "O" Number 2
15	Jake's Valley Number 1
16	Indian Springs Federal Number 22A
17	Cedar Creek Number 2-1
18	Twin Springs Federal Number 10-6
19	Dobbin Creek Federal A No. 1-6
20	Big Smoke No. 1420

Well data sources:

1-8	DeCelles and Coogan (2006)
9-11	Utah Department of Natural Resources (2017)
12-20	Hess et al. (2004)

Rock units:

Intrusive igneous rocks:

- Ki Cretaceous intrusive rocks
- JRi Jurassic intrusive rocks
- JRKi undifferentiated Jurassic to Cretaceous intrusive rocks

Eastern California and Western Nevada:

- QNG Neogene-Quaternary valley fill sediment
- unconformity
- NGs Neogene (late Miocene) sedimentary rocks
- NGv Neogene (early-middle Miocene) volcanic rocks
- PGv Paleogene (Oligocene) volcanic rocks
- unconformity
- JR Jurassic sedimentary and volcanic rocks
- TR Triassic sedimentary and volcanic rocks
- TRJR undifferentiated Triassic and Jurassic sedimentary and volcanic rocks

Allochthonous rocks in Central Nevada:

- MIPPh Mississippian-Pennsylvanian-Permian Havallah Formation (Golconda allochthon) — GT
- Ov Ordovician Vinini Formation (Roberts Mountains allochthon) — RMT

Eastern Nevada and Westernmost Utah:

- QNG Neogene-Quaternary valley fill sediment
- unconformity
- PGv Paleogene (dominantly late Eocene-Oligocene) volcanic and sedimentary rocks
- unconformity
- K Early Cretaceous synorogenic sedimentary rocks (Newark Canyon Formation)
- unconformity
- TR Triassic sedimentary rocks
- P Permian sedimentary rocks
- IP Pennsylvanian sedimentary rocks
- M Mississippian sedimentary rocks
- D Devonian sedimentary rocks
- S Silurian sedimentary rocks
- O Ordovician sedimentary rocks
- Cu Middle-Upper Cambrian sedimentary rocks
- Cl Lower Cambrian sedimentary rocks
- Z Neoproterozoic sedimentary rocks

Western Utah (modified from DeCelles and Coogan, 2006):

- QNGPG Paleogene-Quaternary (Oligocene and younger) valley fill sediment
- unconformity
- PGs Paleogene (Paleocene-early Eocene) synorogenic sedimentary rocks
- unconformity
- K Cretaceous syn-orogenic sedimentary rocks
- JRu Middle-Upper Jurassic syn-orogenic sedimentary rocks
- TRJRl Triassic-Lower Jurassic sedimentary rocks
- MIPP Mississippian-Permian sedimentary rockscks
- CuOSD Middle Cambrian to Devonian sedimentary rocks
- ZCl Neoproterozoic-Lower Cambrian sedimentary rocks

Footnotes keyed to cross section:

1 - Points Z and Z' represent matching positions in the footwall and hanging wall of the SDD, respectively. On the restored section, the location of point Z was used to delineate the restored position of the eastern limit of the Sevier Desert Basin.
2 - The Jurassic Notch Peak granite pluton is exposed ~2 km to the south of the section line; here it is schematically projected in the subsurface.
3 - After Greene (2014), the Knoll anticline and Buckskin Hills syncline are modeled as fault-bend folds that formed above a hanging wall ramp in the Brown's Wash thrust, and the Buckskin Hills anticline is modeled as a detachment fold that formed from displacement transfer above the Brown's Wash thrust (as a consequence, slip magnitude on the Brown's Wash thrust decreases upward and toward the east). The geometry of the detachment fold is approximate, and strucural thickening of Mississippian rocks in the core of the fold is schematically represented here.
4 - The ~23-30 km peak burial depth range of NSRD footwall rocks (from Cooper et al., 2010) is shown at depth. The NSRD is projected to these depths at dip angles ranging from 20° to 40°, based on: 1) The present-day ~25-30° E dip to depths of ~15 km on the COCORP profile (Allmendinger et al., 1983); 2) Evidence for up to 40° of rotation of NSRD footwall rocks during rolling hinge-type exhumation (Lee, 1995); and 3) The 20° origination angle of the NSRD in the middle crust on the structural model of Bartley and Wernicke (1984). Projecting the NSRD to the range of burial depths yields an offset magnitude of 34 ± 13 km on the NSRD, and an E-W extension magnitude of 30 ± 14 km.
5 - The footwall of the NSRD was restored using the 250% extension estimate of Lee et al. (1987), which was based on integration of finite strain data from Neoproterozoic-Cambrian rocks with a comparison of the attenuated thickness of the Cambrian Prospect Mountain Quartzite to its undeformed regional thickness. E-W widths were restored using this extension value, and thicknesses were restored to the 1.2 km regional thickness observed for Lower Cambrian rocks (Miller et al., 1983), and the 5.0 km (minimum) thickness of Neoproterozoic rocks (from exposures in the Deep Creek Range, ~100 km along-strike to the north (Stewart, 1980). Rocks in the footwall of the NSRD are shown restored to stratigraphic depths of ~7-13 km, after the structural model of Miller et al. (1983).
6 - The pre-extensional width of the NSRD hanging wall was estimated by restoring all fault-bound blocks that contain Ordovician, Silurian, and Devonian rocks as close together as possible without overlapping. This represents the minimum possible E-W restored width of the NSRD hanging wall.
7 - The Paleogene unconformity in the Snake Range is shown as bedding-parallel and lying within the Permian section, as Permian rocks are the highest pre-extensional stratigraphic level preserved in multiple across-strike localities within ~5 km to the north and south of the section line (Miller et al., 1999B; Johnston, 2000). The pre-extensional dip angles of Paleozoic rocks are not known. However, ~35 km along-strike to the north, Permian rocks are exposed beneath the Paleogene sub-volcanic unconformity, with minimal (<5°) angular discordance beneath Oligocene volcanic rocks (Gans and Miller, 1983), which supports low pre-extensional dip angles for Paleozoic rocks.
8 - A 4.5 km thickness of Neoproterozoic-Lower Cambrian sedimentary rocks is shown here. This thickness of rocks is observed, undisturbed by faulting, on the eastern flank of the Schell Creek Range ~15 km along-strike to the north (Young, 1960; Gans et al., 1985). These rocks are shown as contiguous below the homoclinally-E dipping Paleozoic section, although the precise dip angle of rocks at this depth cannot be determined.
9 - Due to the large scale of the cross section, these low cutoff-angle, down-to-W normal faults, which bound slices of Cambrian and Ordovician rocks between ~100-400 m thick, are simplified and shown merging into one master fault plane above and below the erosion surface.
10 - The master down-to-west normal fault was projected to the east above the erosion surface with a ~50° footwall cutoff angle, in order to match the hanging wall cutoff angle observed in the range. Its geometry is modeled as a down-to-west listric fault, which has a ~50° stratigraphic cutoff angle through Cambrian-Permian rocks, and a flat near the base of the Cambrian section. The footwall stratigraphy was projected high enough so that point X restores to point X'. This geometry is simplified, and does not account for any down-to-east offset of the range-bounding fault on the east side of the range. However, this is internally consistent with how all ranges were restored (i.e., only faults exposed in the ranges are restored).
11 - A three-point problem (Table DR1) constrains the dip of this down-to-W normal fault that omits much of the Middle-Upper Cambrian section to 15°W.
12 - A three-point problem (Table DR1) constrains the dip of this down-to-W normal fault that places Ordovician rocks over Cambrian rocks to 14°W.
13 - Multiple exposures of this normal fault bounding the base of several klippe of Pennsylvanian rocks constrains the fault dip to 5° E. Restoration of tilting of Paleogene rocks indicates that this fault dipped ~15° W prior to extension.
14 - The presence of normal faults that pre- and post-date the Paleogene unconformity in the Egan Range makes estimation of paleo-horizontal prior to extension difficult. Here, the Paleogene unconformity in the eastern and western parts of the range is restored to horizontal. However, in the hanging wall of the pre-volcanic Kaibab fault, the unconformity restores to a westward dip.
15 - A 3-point problem yielded a dip of 45° W (Table DR1) for this W-dipping normal fault in the eastern part of the Egan Range.
16 - A 3-point problem yielded a dip of 9° W (Table DR1) for the Kaibab fault in the central part of the Egan Range. Field relationships ~5 km to the north of the section line show that the Kaibab fault is overlapped by the Paleogene unconformity (Brokaw and Barosh, 1968), by rocks as young as ~37.5 Ma (Gans et al., 2001).
17 - Humphrey (1960) mapped the Mississippian-Pennsylvanian contact here as the W-dipping Illipah thrust. However, there is no evidence for thrust-sense offset at this latitude, as a complete thickness of E-dipping Mississippian rocks transitions eastward into E-dipping Pennsylvanian rocks. Therefore, no structure is shown here.
18 - An E-vergent thrust fault mapped by Humphrey (1960) places W-dipping Mississippian Chainman shale over E-dipping Pennsylvanian Ely limestone. It is shown with a flat at the base of the Mississippian Chainman shale in the subsurface, and is shown ramping eastward through Pennsylvanian and Permian rocks at and above the erosion surface, as this fault is not observed in the eastern limb of the Illipah anticline.
19 - All 1st-order normal faults in the Diamond Mountains, Fish Creek Range, and Mahogany Hills are intepreted to have accomplished all of their offset during the Late Cretaceous-Paleocene (~75-60 Ma; Long et al., 2015). Because the Paleogene unconformity post-dates extension, it is therefore not restored to horizontal. Rocks in these three ranges were retro-deformed to account for ~20-30° of tilting of Late Cretaceous-late Eocene conglomerate that pre-dates (or was contemporary with) motion on the Pinto Summit fault (Long et al., 2014A). The lowest structural level of the basal unconformity of the Newark Canyon Formation in the hinge zone of the Pinto Creek syncline was restored to a pre-extensional elevation of 3 km.
20 - The RMT in the Fish Creek Range is shown ramping eastward through Mississippian rocks, tipping out at the top of the Mississippian section, and being overlapped by Permian rocks, based on field relations observed ~15 km to the N (Bentz, 1983) and along the section line (Nolan et al., 1974).
21 - The RMT in the Mahogany Hills is shown overlying a ~300 m-thick section of Mississippian rocks, after field relations observed ~15 km to the N (Bentz, 1983). The thickness of Ov is shown as 1600 m, based on the minimum thickness reported ~50 km to the N in the Roberts Mountains (McKee and Conrad, 1998).
22 - This 1st-order, shallowly-dipping (3-point problem: 18° W; Table DR1), down-to-W normal fault in the Mahogany Hills is overlapped by the Paleogene unconformity, and is interpreted to be related to Late Cretaceous-Paleocene normal fault systems exposed to the east in the Fish Creek Range, including the Reese and Berry detachment system (Long et al., 2014A; 2015).
23 - In the eastern half of the Monitor Range, between ~0-10 km S of the cross-section line, the Paleogene unconformity overlies progressively older strata toward the east, including Silurian and Ordovician rocks on the eastern flank of the range (Bortz, 1959; Stewart and Carlson, 1978). The unconformity is therefore projected to lie within these stratigraphic levels.
24 - Two exposures of the RMT, which both carry unit Ov, are exposed in the eastern Monitor Range (Bortz, 1959). They are separated by a thrust fault that carries Ordovician sedimentary rocks of the continental shelf. This thrust fault is shown cutting and duplicating the RMT, and is correlated with an east-vergent thrust fault that places Ordocivian rocks over Silurian rocks mapped in the western part of the range (Lohr, 1965).
25 - A three-point problem constrains the dip of this E-vergent thrust fault that places Ordovician over Silurian rocks in the Monitor Range to 10°E (Table DR1).
26 - This Ordovician-over-Devonian thrust fault mapped in the footwall of the RMT in the Toqiuma Range (McKee, 1976) is shown soling westward into a flat within the Ordovician section, and is shown cutting the RMT above the erosion surface. This thrust, along with two others, are mapped as merging with the RMT ~5-10 km south of the section line (McKee, 1976), and thus could represent footwall imbrication during RMT emplacement.
27 - Five three-point problems constrain the average dip of the Paleogene unconformity in the Toiyabe Range to 15° W (Table DR1).
28 - W-vergent folds and E-dipping thrust faults support modeling the deformation front of the LFTB in the Shoshone Mountains as a W-vergent triangle zone. From east to west, mapping indicates: 1) a W-vergent fold with an overturned lower limb, which is interpreted to have formed above a W-vergent thrust fault at depth; and 2) steeply E-dipping Triassic and Jurassic rocks being carried by W-vergent thrust faults in the western part of the range.
29 - Unit MIPPh is interpreted to underlie Triassic rocks in the Shoshone Mountains, based on exposures mapped ~15 km to the N, and in multiple localities within ~35 km to the S and SW (Stewart and Carlson, 1978; Kleinhampl and Ziony, 1985). The GT is shown at the base of unit MIPPh, and this unit is shown at the same thickness as observed in the Toiyabe Range to the east.
30 - A three-point problem yields a dip of 12°W for the Gabbs thrust in the Paradise Range (Table DR1).
31 - A three-point problem yields a dip of 12°W for the Paraside fault in the Paradise Range (Table DR1). Paleogene-Neogene rocks truncate downward into a gently W-dipping normal fault in the NE part of the Paradise Range that is here correlated with the Paradise fault mapped in the central part of the range by Silberling and John (1989).
32 - Along the section line, many Triassic-Jurassic stratigraphic units are grouped together, dips commonly change over short distances from upright to overturned, implying common meso-scale folding, and large areas of Triassic-Jurassic exposures contain no measurements. Therefore, all Triassic-Jurassic units in the Paradise Range are here shown as undifferentiated, and no attempt was made to illustrate their structural geometry.
33 - No attempt was made to retro-deform dextral offset on strike-slip faults of the central Walker Lane that trend through the Gabbs Valley and Gillis ranges. Instead, the packages of rock between these strike-slip faults were un-tilted and retro-deformed using a similar technique to all other ranges.
34 - In the Gillis Range, all contacts between Cenozoic and pre-Cenozoic rocks were mapped by Hardyman (1980) as low-angle normal fault contacts. No information on their kinematics are available, but Hardyman (1980) interpreted them to be genetically related to dextral strike-slip faulting. Here, these low-angle faults are simplified to one gently E-dipping fault plane. This fault cuts gently down-section toward the east, implying a component of down-to-east motion. However, as the kinematics of this fault in and out of the plane of the cross section are unknown, offset on this fault was not incorporated into the estimation of extension. Also, Eckberg et al. (2005) disputed several of these low-angle faults, and instead mapped them as unconformities.
35 - Several 1st-order, shallowly E-dipping normal faults in the Wassuk Range have to dip at least 12-14°E to not intersect the modern erosion surface to the west or east of their traces. This requires high cutoff angles (~60-70°) with Paleogene-Neogene volcanic rocks, which requires high origination angles (e.g., Surpless et al., 2002).
36 - Several 1st-order, shallowly E-dipping normal faults in the Buckskin Range must dip at least 12-13°E to not intersect the modern erosion surface to the east of their traces. This requires high cutoff angles (~70°) with Neogene volcanic rocks, and high origination angles (Proffett, 1977). The Singatse fault is constrained to a 2°E dip by interactions of its trace with topography.

B. Restored

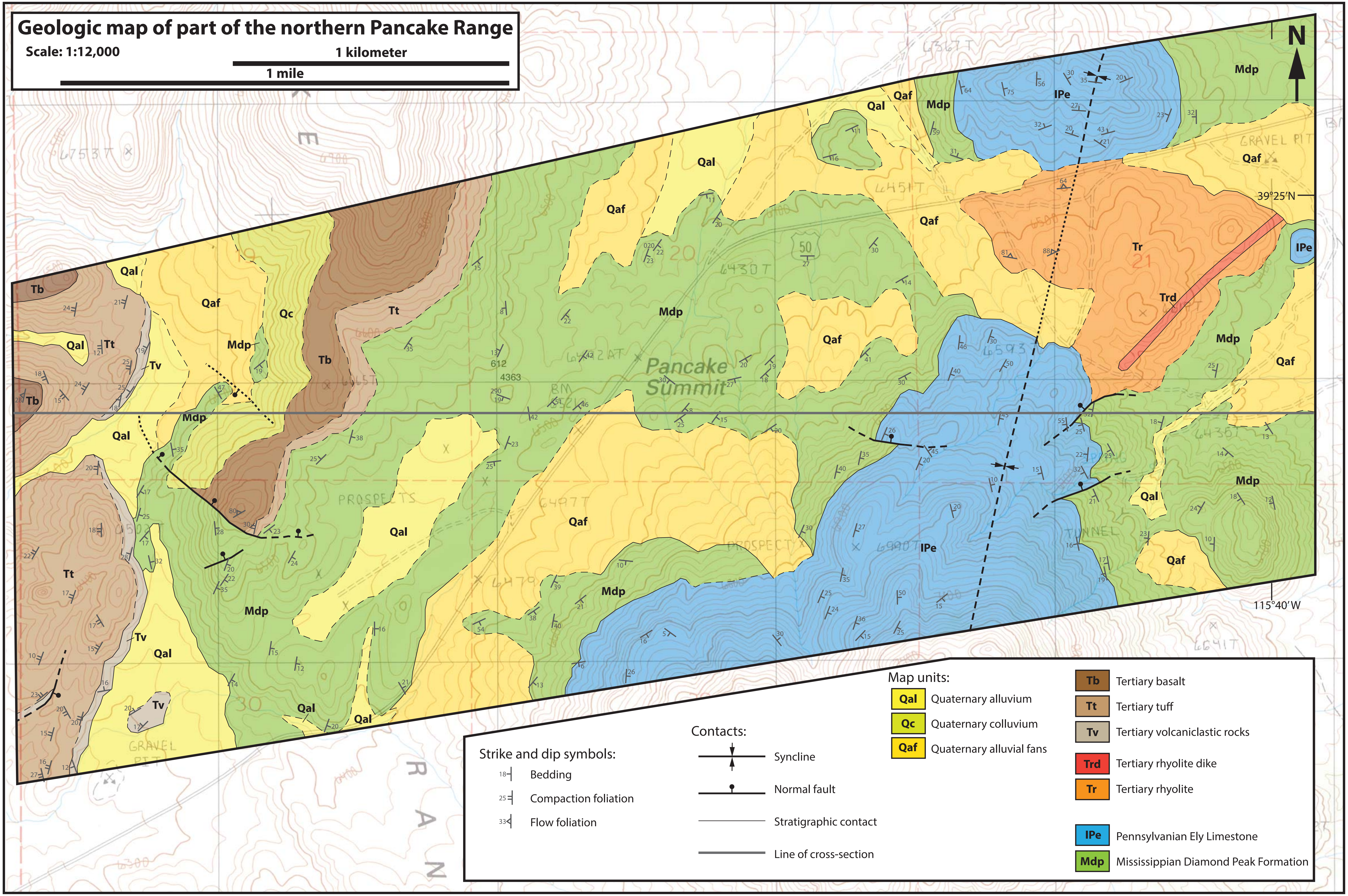
Geologic map of part of the northern Pancake Range
Scale: 1:12,000
1 kilometer
1 mile
N
39°25'N
115°40'W
Pancake Summit
PROSPECTS
PROSPECT
TUNNEL
GRAVEL PIT
Map units:
Qal Quaternary alluvium
Qc Quaternary colluvium
Qaf Quaternary alluvial fans
Tb Tertiary basalt
Tt Tertiary tuff
Tv Tertiary volcaniclastic rocks
Trd Tertiary rhyolite dike
Tr Tertiary rhyolite
IPe Pennsylvanian Ely Limestone
Mdp Mississippian Diamond Peak Formation
Contacts:
Syncline
Normal fault
Stratigraphic contact
Line of cross-section
Strike and dip symbols:
Bedding
Compaction foliation
Flow foliation

Location and fault	Geologic mapping source	Strike azimuth	Elevation difference	Horizontal distance	Fault dip angle
Schell Creek Range, easternmost low-angle normal fault	Drewes (1967)	008°	160'	600'	15° W
Schell Creek Range, low-angle normal fault (2nd from east)	Drewes (1967)	353°	200'	800'	14° W
Egan Range, 2nd-order W-dipping normal fault	Brokaw (1967)	330°	200'	200'	45° W
Egan Range, Kaibab fault	Brokaw and Heidrick (1966)	341°	80'	500'	9° W
Mahogany Hills, 1st-order W-dipping normal fault	Schalla (1978)	338°	180'	550'	18° W
Monitor Range, E-dipping thrust fault	Lohr (1965)	353°	480'	2800'	10° E
Toiyabe range, Paleogene unconformity (1)	Ferguson and Cathcart (1954)	010°	2000'	12400'	9° W
Toiyabe range, Paleogene unconformity (2)	Ferguson and Cathcart (1954)	023°	2400'	10400'	13° W
Toiyabe range, Paleogene unconformity (3)	Ferguson and Cathcart (1954)	008°	1200'	4800'	14° W
Toiyabe range, Paleogene unconformity (4)	Ferguson and Cathcart (1954)	023°	1200'	4100'	16° W
Toiyabe range, Paleogene unconformity (5)	Ferguson and Cathcart (1954)	027°	1500'	3400'	24° W
Paradise Range, Gabbs thrust	Silberling and John (1989)	002°	1100'	5800'	12° W
Paradise Range, Paradise fault	Silberling and John (1989)	354°	700'	3200'	12° W